

## Proton–Proton Constraints in Powdered Solids from $^1\text{H}$ – $^1\text{H}$ – $^1\text{H}$ and $^1\text{H}$ – $^1\text{H}$ – $^{13}\text{C}$ Three-Dimensional NMR Chemical Shift Correlation Spectroscopy

Dimitris Sakellariou, Anne Lesage, and Lyndon Emsley\*

Laboratoire de Stéréochimie et des Interactions Moléculaires  
UMR 5532 CNRS/ENS-Lyon, École Normale Supérieure  
de Lyon, 46 Allée d'Italie, 69364 Lyon, France

Received December 4, 2000

Revised Manuscript Received April 27, 2001

High-resolution  $^1\text{H}$  spectra of powdered organic molecules represent a potentially rich source of structural and dynamic information in a wide range of materials, from inorganic catalysts to proteins, and their obtention has always been a challenge for the solid-state NMR community.<sup>1</sup> Under magic angle spinning (MAS) conditions,  $^1\text{H}$  resolution is dominated by residual (unaveraged)  $^1\text{H}$ – $^1\text{H}$  dipolar couplings. One approach to improving resolution is isotopic dilution (using deuteration),<sup>2</sup> but this method cannot be routinely applied. Recently, significant progress has been made with the introduction of multiple quantum approaches under MAS,<sup>3,4</sup> and with the improvement in homonuclear dipolar decoupling sequences used under Combined Rotation And Multiple Pulse (CRAMPS) conditions. Notably, two recently introduced windowless homonuclear decoupling schemes<sup>5,6</sup> appear, using indirect detection and relatively rapid MAS rates, to give sufficient resolution to routinely distinguish between proton resonances having chemical shift differences as small as 0.5 ppm in rigid solids.

With this increase in resolution, one can envisage adapting to protons some of the multidimensional techniques used widely in liquid-state NMR and for rare nuclei in solid-state NMR. These techniques should allow the assignment of  $^1\text{H}$  spectra and subsequently allow access to structural and dynamic information via, notably, chemical shifts, chemical shift anisotropies, or dipolar couplings. Perhaps the most exciting possibility is that of measuring  $^1\text{H}$ – $^1\text{H}$  dipolar correlations in solids,<sup>4</sup> thereby providing structural constraints similar to those used to determine structure in liquid-state NMR. In this communication we present two three-dimensional correlation sequences which can be applied to organic solids, and which demonstrate how high-resolution  $^1\text{H}$ – $^1\text{H}$  dipolar correlations can be measured. In both cases proton–proton and proton–carbon correlations are obtained by dipolar driven spin diffusion. The methods are demonstrated on a dipeptide sample.

In the following we use the denomination “CRAMPS” to signify indirectly detected CRAMPS spectra obtained using relatively fast MAS. The first method correlates two high-resolution CRAMPS  $^1\text{H}$  spectra with the standard  $^1\text{H}$  MAS spectrum, and the pulse sequence is given in Figure 1a. The sequence is a phase-sensitive 3D analogue of the 2D CRAMPS–MAS correlation sequence recently introduced by Vinogradov et al.<sup>5</sup> During  $t_1$  and  $t_2$  homonuclear proton decoupling is applied and the magnetization rotates around the effective field of the sequence with a scaled Zeeman interaction. The first  $\pi/2$  pulse places the magnetization perpendicular to the effective field. After

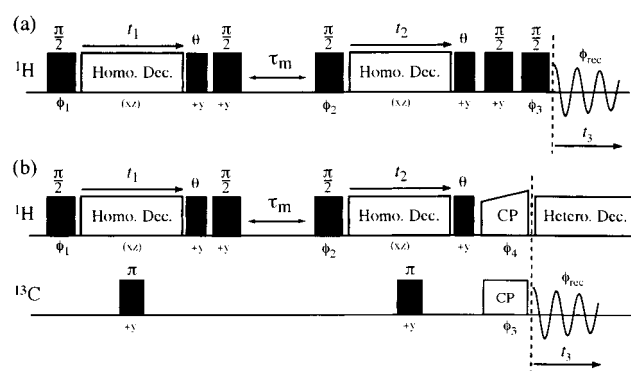


**Figure 1.** (a) Pulse sequence for  $^1\text{H}$ – $^1\text{H}$ – $^1\text{H}$  phase sensitive three-dimensional correlation solid-state CRAMPS NMR spectroscopy. (b) Sequence for  $^1\text{H}$ – $^1\text{H}$ – $^{13}\text{C}$  3D correlation spectroscopy. Various decoupling schemes can be applied. We used the FSLG<sup>7</sup> homonuclear decoupling scheme and the TPPM<sup>8</sup> heteronuclear decoupling scheme. The pulse sequences are available on our website,<sup>9</sup> or upon request.

the  $t_1$  period, the magnetization is placed in the  $xy$  plane of the laboratory frame by the  $\theta$  prepulse. A subsequent  $\pi/2$  pulse stores the magnetization along the laboratory  $z$  axis where polarization exchange takes place during a mixing period  $\tau_m$  (synchronized to be an integral number of rotor periods). During this period no homonuclear decoupling is present and proton spin diffusion occurs driven by the residual dipolar couplings under MAS. The proton magnetization is then placed perpendicular to the effective field for a second evolution period  $t_2$ . Finally, the signal is acquired during  $t_3$  under standard MAS conditions. Quadrature detection is achieved in  $t_1$  and  $t_2$  using either the States or TPPI methods by varying the phase of the  $\pi/2$  pulse following each evolution period. (All the pulse sequences are available on our website.<sup>9</sup>)

This sequence allows one to obtain a high-resolution 2D proton–proton correlation spectrum using high-performance windowless homonuclear decoupling schemes. It is analogous to a two-dimensional version proposed in the literature with windowed decoupling<sup>10</sup> which was used previously to measure intermolecular proton spin diffusion between different polymer domains, occurring over long mixing times (several ms), and where the resolution was sufficient only to distinguish between grossly different types of proton (e.g. aromatic–aliphatic).<sup>10</sup> In the 3D version the projection onto the  $F_1$ – $F_2$  axis, shown in Figure 2 for a natural abundance sample of powdered L-Analyt-L-aspartic acid, has sufficient resolution to measure intramolecular correlations between the different protons in the molecule (with  $\tau_m = 320 \mu\text{s}$ ). The intensity of the proton–proton correlations is related to the internuclear separation. The spectrum contains 6 resolvable proton resonances, which have been assigned previously.<sup>11</sup>

We note that the third dimension in this experiment, which is simply the standard proton MAS spectrum, is largely redundant. Thus, to increase the information content of these spectra, and to fully profit from the three-dimensional nature of the experiment, we propose the  $^1\text{H}$ – $^1\text{H}$ – $^{13}\text{C}$  correlation sequence presented in Figure 1b. The first part of the sequence, containing  $t_1$  and  $t_2$ , is identical to the previous sequence. After  $t_2$ , a cross polarization

(1) Haeberlen, U. *High-Resolution NMR in Solids: Selective Averaging*, Adv. Magn. Reson. Suppl. 1; Academic Press: New York, 1976.

(2) Zheng, L.; Fishbein, K. W.; Griffin, R. G.; Herzfeld, J. *J. Am. Chem. Soc.* **1993**, *115*, 6254.

(3) Graf, R.; Demco, D. E.; Gottwald, J.; Hafner, S.; Spiess, H. W. *J. Chem. Phys.* **1997**, *106*, 885.

(4) Schnell, I.; Brown, S. P.; Low, H. Y.; Ishida, H.; Spiess, H. W. *J. Am. Chem. Soc.* **1998**, *120*, 1178.

(5) Vinogradov, E.; Madhu, P. K.; Vega, S. *Chem. Phys. Lett.* **1999**, *314*, 443.

(6) (a) Sakellariou, D.; Lesage, A.; Hodgkinson, P.; Emsley, L. *Chem. Phys. Lett.* **2000**, *319*, 253. (b) Sakellariou D.; Emsley, L. Manuscript in preparation.

(7) (a) Bielecki, A.; Kolbert, A. C.; Levitt, M. H. *Chem. Phys. Lett.* **1989**, *155*, 341. (b) Bielecki, A.; Kolbert, A. C.; De Groot, H. J. M.; Griffin, R. G.; Levitt, M. H. *Adv. Magn. Reson.* **1990**, *14*, 111.

(8) Bennett, A. E.; Rienstra, C. M.; Auger, M.; Lakshmi, K. V.; Griffin, R. G. *J. Chem. Phys.* **1995**, *103*, 6951.

(9) <http://www.ens-lyon.fr/STIM/NMR>.

(10) Caravatti, P.; Neunschwander, P.; Ernst, R. R. *Macromolecules* **1985**, *18*, 119.

(11) Gu, Z.; Ridenour, C. F.; Bronnimann, C. E.; Iwashita, T.; McDermott, A. *J. Am. Chem. Soc.* **1996**, *118*, 822.

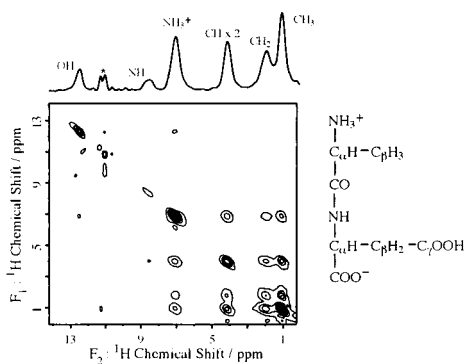


**Figure 2.**  $F_1$ - $F_2$  projection of the 3D homonuclear proton correlation spectrum for a powder sample of L-Alanyl-L-aspartic acid. The one-dimensional spectrum shown above the 2D map corresponds to the indirectly detected CRAMPS  $^1\text{H}$  spectrum. There is a zero frequency artifact arising from imperfect calibration of the  $\theta$  prepulse, indicated by a star. The spectra were obtained on a Bruker DSX 500 MHz spectrometer, using a 4 mm triple resonance CPMAS probe. The sample was restricted to the central  $1/3$  of the rotor. The total spectral width in  $F_1$  and  $F_2$ , after correction for the experimental scaling factor  $\lambda = 0.5$ , was  $\sim 30$  kHz, with  $\nu_1^{\text{H}} = 100$  kHz and  $\nu_r = 12.5$  kHz. Eight scans were acquired for 128 by 128 points in  $t_1$  and  $t_2$ , using a repetition time of 1 s.

step transfers proton coherence to the neighboring carbons, with an efficiency that depends on the geometry of the spin system, the cross-polarization mixing time, and the spin dynamics of CP, as has been extensively discussed in the literature.<sup>12</sup> Subsequently, the carbon signal is observed under heteronuclear decoupling. A  $\pi$  pulse is applied to carbon in the center of  $t_1$  and  $t_2$  to remove the effect of heteronuclear scalar couplings.<sup>13</sup>

This experiment correlates the two high-resolution  $^1\text{H}$  CRAMPS spectra with the high-resolution  $^{13}\text{C}$  spectrum, thereby exploiting the large chemical shift dispersion of  $^{13}\text{C}$  in the third dimension. Figure 3 presents the  $F_1$ - $F_2$  slices of the  $^1\text{H}$ - $^1\text{H}$ - $^{13}\text{C}$  experiment taken at different isotropic carbon chemical shifts for the dipeptide. For a given slice, "diagonal" peaks correspond to magnetization that had the same frequency during  $t_1$  and  $t_2$ , and which has been transferred to the carbon whose chemical shift defines the slice. Off-diagonal peaks correspond to magnetization that has been exchanged between  $^1\text{H}$  sites between  $t_1$  and  $t_2$  and transferred during the cross polarization step to the carbon. If the heteronuclear transfer was fully selective, i.e., occurring only between chemically bonded CH pairs, strips along  $F_2$  should be observed. This is not the case in the spectra presented here (with a  $150 \mu\text{s}$  CP step), and thus the spectrum contains information about nearby  $^1\text{H}$ - $^1\text{H}$  and  $^1\text{H}$ - $^{13}\text{C}$  connectivities. For example, in the case of the dipeptide this 3D experiment allows us to resolve the proton-proton correlations for the two CH protons, which are not resolved in the 1D  $^1\text{H}$  CRAMPS spectrum. We see from the slices in Figure 3 that one of these protons correlates very strongly with both the  $\text{CH}_3$  protons and the  $\text{NH}_3^+$  protons. This allows us to assign this C-H pair to that of the Ala residue and the other CH resonance to that of the Asp residue. Similarly, we observe a strong correlation between a CO carbon resonance and the OH and  $\text{CH}_2$  protons, allowing the assignment of this carbon as  $\text{C}_\gamma\text{O}$ .

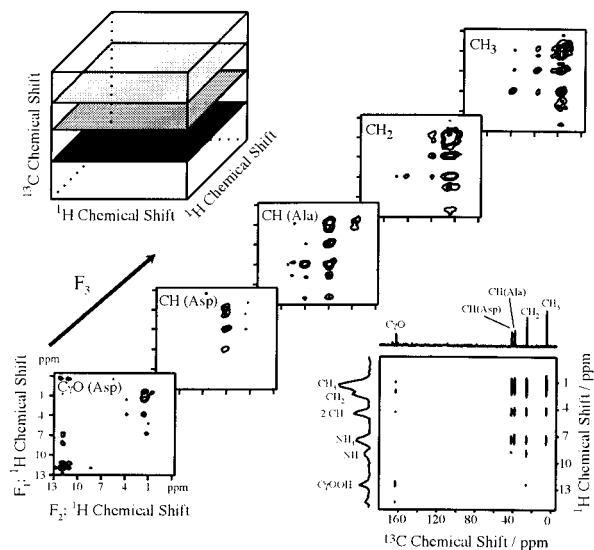


**Figure 3.** Three-dimensional  $^1\text{H}$ - $^1\text{H}$ - $^{13}\text{C}$  spectrum of Ala-Asp.  $F_1$ - $F_2$  slices are extracted along the  $F_3$  dimension at the isotropic carbon resonances. Sixteen scans were acquired for each of 80 by 80 points in  $t_1$  and  $t_2$ , using a repetition time of 2 s. The 3D data were acquired in  $\sim 57$  h. All other experimental conditions were the same as for Figure 2.

Of course, 3D experiments have previously been proposed in solids. In particular, high-resolution 3D proton-proton chemical shift correlation spectroscopy has been performed in oriented media (single crystals)<sup>14</sup> or in elastomers<sup>15</sup> and the experiments we present here are the first of this type suitable for powdered rigid organic samples. Note also that many variants of this experiment are imaginable. For example, the heteronuclear polarization transfer step can use either dipolar<sup>16</sup> (as in our example) or scalar couplings<sup>17</sup> and the heteronucleus can be any NMR accessible rare nucleus, notably  $^{15}\text{N}$  or  $^{31}\text{P}$ .

In conclusion, we have presented two three-dimensional correlation experiments that make use of the high proton resolution obtained using indirectly detected CRAMPS. They yield detailed information regarding the assignment and the structure of powdered organic molecules, notably about proton connectivities. Previously, structure determination in solids has relied mostly on C-C and C-N distances. The spectra we present here clearly indicate the viability of measuring  $^1\text{H}$ - $^1\text{H}$  distance constraints in solids, introducing experiments directly analogous to the ubiquitous NOESY experiment in liquids. In general, information about the environment of hydrogen nuclei can only be obtained in the solid state using neutron diffraction methods. The sequences we propose here can be used as building blocks in the development of more sophisticated multinuclear and multidimensional solid-state NMR experiments.

JA005846H

(14) (a) Ramamoorthy, A.; Gierasch, L. M.; Opella, S. J. *J. Magn. Reson. B* **1996**, *111*, 81. (b) Ramamoorthy, A.; Wu, C. H.; Opella, S. J. *J. Magn. Reson.* **1999**, *140*, 131.

(15) Fritzhanns, T.; Demco, D. E.; Hafner, S.; Spiess, H. W. *Mol. Phys.* **1999**, *97*, 931.

(16) Van Rossum, B. J.; Forster, H.; De Groot, H. J. M. *J. Magn. Reson.* **1997**, *124*, 516.

(17) Lesage, A.; Sakellariou, D.; Steuernagel, S.; Emsley, L. *J. Am. Chem. Soc.* **1998**, *120*, 13194.

(12) Meier, B. H. *Adv. Magn. Reson.* **1994**, *18*, 1.

(13) Lesage, A.; Emsley, L. *J. Magn. Reson.* **2001**, *148*, 449.